Interaction modes between asymmetrically and oppositely charged rods

Hanne S. Antila,[1] Paul R. Van Tassel,[2] and Maria Sammalkorpi[1,*]
[1]*Department of Chemistry, Aalto University, FI-00076 Aalto, Finland*
[2]*Department of Chemical & Environmental Engineering, Yale University, New Haven, Connecticut 06520, USA*
(Received 2 September 2015; published 5 February 2016)

The interaction of oppositely and asymmetrically charged rods in salt—a simple model of (bio)macromolecular assembly—is observed via simulation to exhibit two free energy minima, separated by a repulsive barrier. In contrast to similar minima in the Derjaguin-Landau-Verwey-Overbeek (DLVO) theory, the governing mechanism includes electrostatic attraction at large separation, osmotic repulsion at close range, and depletion attraction near contact. A model accounting for ion condensation and excluded volume is shown to be superior to a mean-field treatment in predicting the effect of charge asymmetry on the free-energy profile.

DOI: 10.1103/PhysRevE.93.022602

I. INTRODUCTION

Charged molecules and ion mediated forces govern the thermodynamics of most aqueous soft matter suspensions [1,2]. A large body of work has addressed systems of colloidal-type particles whose charges are all of the same sign; see, e.g., [1,3–9]. However, realistic solutions often contain oppositely charged units, e.g., DNA complexes, supramolecular protein aggregates, intracellular viruses, and polyelectrolyte assemblies. For the systems mentioned above, charged rods are natural coarse-grained representation, but to our knowledge, the interaction of oppositely charged rods in aqueous solutions has not been examined previously via simulation. Even for other geometries, studies on oppositely charged objects [10–17] are less common than their like-charge counterparts.

The relative neglect of systems containing oppositely charged macroions may stem from the intuitive, but misplaced, preconception that they would be intrinsically unstable, and do not present interesting phase behavior. Indeed, utilizing most traditional approaches, like the Debye-Hückel [18] or the Derjaquin-Landau-Verwey-Overbeek (DLVO) [19,20] theories with the common superposition approximation, typically results in electrostatic attraction, screened by added electrolyte, between oppositely charged objects [21,22]. However, the full Poisson-Boltzmann (PB) equation can predict a short range repulsion when the two macroions are nonequally (asymmetrically) charged. Considering again the large variety of charged surfaces occurring in biological context, this effect of charge asymmetry is of interest. The repulsion stems from the osmotic pressure associated with the ionic atmosphere around the charged colloids and has been demonstrated for two oppositely and charged spheres [10,11], plates [10,12,17], or cylinders [23] in the context of the mean-field PB equation. In the planar geometry, this behavior has also been observed in experiments [24].

Beyond the mean-field approximation, one encounters the so-called weak and strong coupling approaches [25–27], which account for non-PB effects by considering charged systems in two limits of electrostatic coupling. Weak coupling involves charge compensating counterions, and salt species, whose spatial distributions are weakly (but not vanishingly) correlated. These spatial effects are treated through a second-order correction to the mean-field PB solution, and the approach is applicable at low colloidal charge and for monovalent ions. In contrast, strong coupling involves ions whose spatial distribution is highly correlated. Ion structures are taken to be those of a ground state (i.e., zero temperature), or perturbations thereof, and the approach is valid at high colloidal charge, high ion valence, and/or low solvent dielectric constant. As with mean-field descriptions, studies of colloidal interactions in the strong coupling regime have mainly concentrated on like-charge interactions [28–32]. An exception is the work by Kanduč *et al.* [33], where simulation and theory of interactions between asymmetrically charged plates, under both strong and weak coupling conditions, were presented. Two interaction regimes were observed: one attractive at all separations, and one attractive at short range but repulsive at longer range. An interesting finding was a decrease in the attraction-repulsion crossover separation with degree of coupling [33].

More generally, effects related to the configuration of the ions around a macroion are known to have a significant effect on macroion-macroion interactions, particularly under strong Coulomb coupling conditions. A well-known example is the counterintuitive attraction between macroions of like charge [34–37], for which the strongly correlated counterion structure [25,29] or the presence of temporal counterion density fluctuations [38] are among the theoretically proposed mechanisms. Interestingly, the depletion of counterions between nearly touching, like-charged macroions has also been shown to cause an attractive interaction [39].

Charged systems exhibit a strong, qualitative dependence on geometry. One example is the mean-field condensation of ions, to an isolated charged surface, due to a balance of Coulomb energetic attraction and release entropy: Full (i.e., charge compensating) condensation occurs in a planar system, partial condensation occurs onto a cylinder, and none occurs onto a sphere. The cylindrical case may be treated in the mean-field via Manning condensation theory [40], and the degree of Coulomb coupling may additionally influence (quantitatively) the degree of charge compensation. Another example is the osmotic pressure exerted by neighboring counterions. The cylindrical and spherical geometries allow for the counterion distribution to become asymmetric and to exert different degrees of osmotic pressure on either side of

*maria.sammalkorpi@aalto.fi

the charged object, or on two (or more) neighboring charged objects, while the planar geometry does not allow for such a possibility. These key differences suggest that geometry significantly affects the interplay of different contributions to the interaction of charged colloidal systems.

The significant influence of the ion structure on the interaction between like-charged macroions motivates us to consider such effects in the case of opposite but asymmetric charge and in cylindrical geometry. Through Monte Carlo simulation, we determine the force between two rod-shaped objects, as a function of charge asymmetry and solution ionic strength, under weak Coulomb coupling conditions. As expected, we observe conditions of (i) pure attraction at all separations and (ii) long-range attraction followed by short-range repulsion, in line with preceding work on asymmetrically charged flat surfaces. However, our key finding is a third possibility: short-range attraction, mid-range repulsion, and long-range attraction, i.e., two attractive regimes separated by a repulsive barrier. The observed attraction-repulsion-attraction regime is due to the asymmetric counterion distribution and gradual depletion of counterions from the intersurface space—both possible in the cylindrical but not the planar geometry—and is accompanied by the formation of a double minima in the free energy profile. While reminiscent of the well-known DLVO double free energy minimum of like-charged objects, the governing physics here is very different.

II. METHODS

Our model system consists of two parallel, oppositely charged rods, C_1 and C_2, of charge per unit length $\tau_1 e$ and $-\tau_2 e$ (with $\tau_2 > \tau_1 > 0$), in a periodic cubic simulation box of length $L = 20 l_B$, where $l_B = e^2/4\pi\varepsilon k_B T$ denotes the Bjerrum length, e the elementary charge, k_B the Boltzmann constant, and T the absolute temperature. While τ_1 is varied, $\tau_2 = 4/l_B$ throughout. The rod radius is $r_0 = 1.1 l_B$. The system also contains $(\tau_2 - \tau_1)L + n_0 L^3$ positively charged and $n_0 L^3$ negatively charged monovalent hard sphere ions of radius $r_I = 0.3 l_B$, where n_0 is the density of added electrolyte, leading to a Debye screening length $\kappa^{-1} = (\varepsilon k_B T/n_0 e^2)^{1/2}$. The water solvent is described by a dielectric continuum of permittivity ε. The system parameters resemble DNA (C_2) and a polycation that changes its charge density via protonation (C_1).

NVT ensemble (Metropolis) Monte Carlo simulations of 10^8 steps are utilized to examine the rod-rod interactions for varying τ_1 and κ. The ions and rods interact via hard-sphere repulsion and Coulombic interactions, modeled by an Ewald summation scheme where the rod charge is represented as a continuous line charge. The sampling is sufficient to ensure the convergence of the calculated total forces on the rods ($F_{\mathrm{tot},i} = F_{\mathrm{el},i} + F_{\mathrm{hs},i}$). Ewald summation provides the electrostatic component F_{el} and the hard-sphere collision forces (F_{hs}) exerted on the rods by the ions are determined based on the ion contact density [41]. Due to asymmetry, the force components for each rod differ, but in accordance with Newton's 3rd law $\sum_i \vec{F}_{\mathrm{tot},i} = 0$ (checked for all systems). Uncertainty of the calculated forces is reflected by the symbol size in the figures.

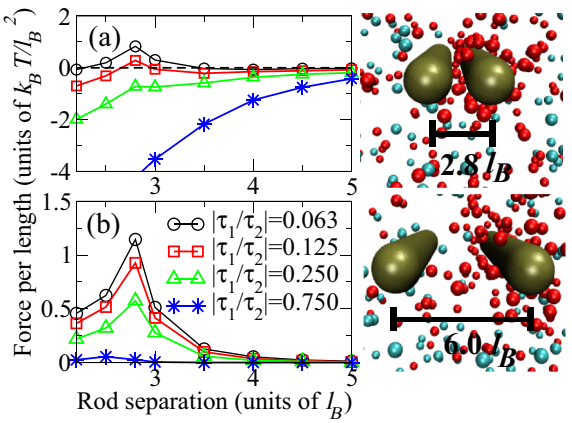

FIG. 1. (a) Total force per length between the rods and (b) osmotic contribution to the force from the cations in the interrod space, for varying rod charge ratio $|\tau_1/\tau_2|$ and κ=0.7 l_B^{-1}. A positive force corresponds to repulsion. At right, simulation snapshots of the system at two rod separations.

III. RESULTS AND DISCUSSION

In Fig. 1, we show the interaction force versus rod separation, for various extents of charge asymmetry, at a slightly sub-physiological 1:1 electrolyte concentration. The charge asymmetry is quantified with rod charge ratio $|\tau_1/\tau_2|$. For low to modest charge asymmetry, the interaction is purely attractive at all separations, as expected. Interestingly, for $|\tau_1/\tau_2| = 0.25$, a local maximum in the (still everywhere attractive) force appears, and for $|\tau_1/\tau_2| = 0.125$, it becomes a repulsive barrier. The barrier appears at $2.8 l_B$, which corresponds to the limiting separation where one layer of ions may reside between the rods. For $|\tau_1/\tau_2| = 0.125$, the rods are attracted to one another on either side of the repulsive peak. The repulsive peak is enhanced by increasing rod charge asymmetry, and the short-range attraction is eventually completely suppressed.

Repulsion arises because the approach of C_1 (lower charge density) induces a perturbation on the ionic cloud around C_2 (higher charge density), resulting in a repulsive electrostatic force on C_2 and a repulsive osmotic force on C_1 due to unbalanced collisions by the cations around C_2. The perturbed cloud also yields a small attractive osmotic force on C_2. The osmotic force on C_1 is at maximum when exactly one layer of ions fits between the rods (see Fig. 1). Increasing charge asymmetry allows more cations to remain condensed around C_2, during the approach by C_1, consequently increasing the osmotic effect. A similar mechanism of repulsion has been detected for asymmetrically and oppositely charged spherical colloids, and even between charged and a neutral colloid [42].

The important new finding here is that the osmotic repulsion becomes reduced, and can give way to a net attraction, as the two rods approach one another to contact (at $2.2 l_B$). Ions "squeeze out" from between the rods under close separation, suppressing the repulsive osmotic interaction. This short-range effect is a manifestation of ion exclusion from the inter-rod space, which promotes depletion attraction in the system [39], and causes an interaction profile with a double free energy minima. Oppositely of this mechanism, the angular distribution of ions at angles facing the other rod has been

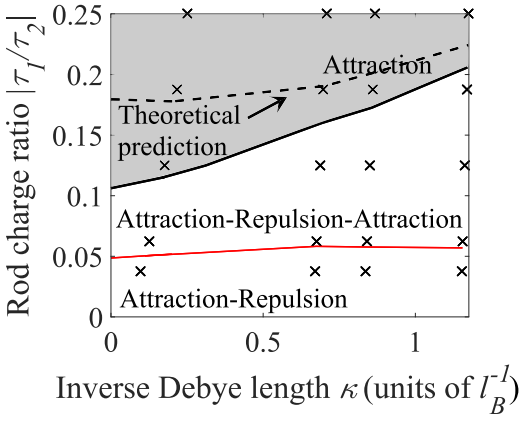

FIG. 2. Interaction "phase diagram" for two oppositely charged rods in terms of rod charge asymmetry ($|\tau_1/\tau_2|$) and inverse Debye length κ. "Attraction" denotes attraction at all separations, "Attraction-Repulsion" long-range attraction with short-range repulsion, and "Attraction-Repulsion-Attraction" a repulsive barrier separating long- and short-range attraction. Linear interpolation between simulated data points (marked by x) is used to determine phase boundaries. Theoretical prediction for the "Attraction"–"Attraction-Repulsion-Attraction" boundary based on Eqs. (3)–(5) is presented as a dashed line.

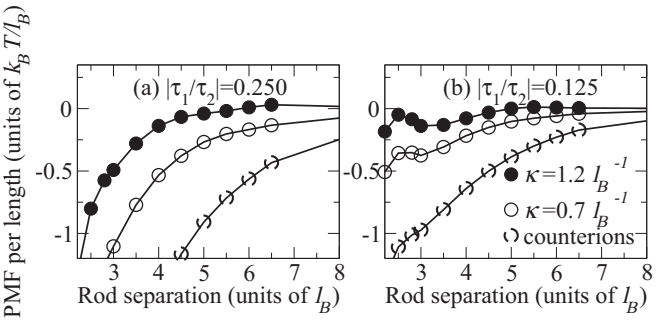

FIG. 3. The potentials of mean force (PMF) per length for rod charge ratios (a) $|\tau_1/\tau_2| = 0.250$ and (b) $|\tau_1/\tau_2| = 0.125$ at different κ.

shown to be of importance in producing attraction between rods of equal charge [36].

The attraction-repulsion-attraction interaction mode is strongly dependent upon system geometry: It cannot be observed in simulations of two infinite plates (see, e.g., [33]) where ions are not depleted from the intersurface space abruptly at a separation equal to their diameter. In this sense, the osmotic pressure in the planar geometry is always highly asymmetric, as ions never come in contact with the outer surfaces.

In Fig. 2, we show an interaction "phase diagram" indicating conditions under which the following behaviors occur: (i) pure attraction, (ii) long-range attraction together with short-range repulsion, and (iii) a repulsive barrier separating long- and short-range attraction. We find increasing *either* rod charge asymmetry or electrolyte concentration to promote a repulsive barrier separating two attractive regimes. Additional salt acts (1) to suppress ion release entropy and to promote ion condensation to the rods, leading to increased osmotic repulsion, and (2) to more effectively screen the Coulombic attraction between the rods; both of these effects favor the repulsive barrier. Further increase in rod charge asymmetry leads to an extent of ion condensation sufficient to yield repulsion at all short-range separations down to contact.

To investigate the effect of salt on the free energy landscape, we show in Fig. 3 a comparison of the potentials of mean force (PMF) at different salt concentrations for $|\tau_1/\tau_2| = 0.250$, which is purely attractive for all concentrations studied here, and $|\tau_1/\tau_2| = 0.125$, where a repulsive barrier is induced by the addition of electrolyte. PMFs are determined by integrating the total average force versus distance, with the zero energy taken at rod separation $10\,l_B$.

All the systems presented in Fig. 3 display a global free energy minimum at contact, i.e., a rod separation of $2.2l_B$. Increasing electrolyte concentration leads to the emergence of a repulsive peak and a secondary, local free energy minimum between 2.5–$3.5l_B$ in the $|\tau_1/\tau_2| = 0.125$ system. Increasing salt concentration also raises the free energy minima, relative to the zero at full separation, and thus may enable reversible binding of macroions. It is interesting to note the high degree of external control over the interaction profile: The repulsive barrier increases with salt concentration, and the position of the peak scales directly to the ion size.

The existence of two binding states, corresponding to the two free energy minima, is a topic of great practical importance from an experimental point of view, and could have important implications to technological applications of macroion complexes. Indeed, highly charged DNA has recently been reported to bind to weakly charged poly(ethyleneimine) (PEI) in both a strongly and weakly bound state [43]. In contrast, the more strongly charged poly(L-lysine) exhibits only a single, tightly bound state with DNA [43]. The presence of a weaker binding state has been suggested [43,44] to be crucial for a polycation to serve as a genetic carrier in gene therapy, as it may enable more effective and controllable release of the DNA from the carrier. This experimental evidence is in line with our results which suggest that this type of polyelectrolyte binding is dependent on charge asymmetry. Furthermore, our data indicate that the binding can be externally regulated by electrolyte concentration and solution pH (which influences the polycation charge).

It is interesting to note the qualitative similarity between the free energy profiles in Fig. 3 and those of the DLVO model of like-charged colloidal objects. In DLVO, the interplay of electrostatic repulsion and van der Waals attraction can induce a secondary attractive well, also controllable by solution ionic strength [45]. An entirely different mechanism is at play in the oppositely and asymmetrically charged systems considered here, where electrostatic and depletion attraction, and osmotic repulsion, conspire to create a double minima free energy profile.

For oppositely and asymmetrically charged rods in the presence of electrolyte, single free energy minima profiles with long-range attraction and short-range repulsion are predicted by the nonlinear Poisson-Boltzmann equation [23],

$$\nabla^2\psi = \kappa^2 \sinh(\psi). \quad (1)$$

Here, the potential ψ has been scaled by e/k_BT. Equation (1) is solved numerically through a finite-element method with a constant surface charge boundary condition and the resulting force, F_{PB}, on a rod is calculated by integrating the stress tensor $\mathbf{T}$ over a surface enclosing the rod. The ij component of the stress tensor is defined as

$$\mathrm{T}_{ij} = 2n_0k_BT(\cosh(\psi)-1) + \tfrac{1}{2}\varepsilon\delta_{ij}\mathbf{E}^2 - \varepsilon E_iE_j, \qquad (2)$$

where indices i and i refer to coordinate directions. The first term of T_{ij} represents the osmotic pressure due to excess electrolyte (compared to bulk solution), and the last two terms belong to the Maxwell stress tensor, δ_{ij} is the Kronecker delta, and $\mathbf{E} = -\frac{k_BT}{e}\nabla\psi$ is the electric field.

In order to predict the repulsive barrier and the double free energy minima observed here, we propose a statistical mechanical model accounting for ion condensation and first-order excluded volume effects. For simplicity, we assume $\tau_2 - \tau_1 \geqslant 1/l_B \geqslant \tau_1 \geqslant 0$, but note that only slightly modified expressions result for other conditions. At small distances D between the rod centers ($\kappa(D-2r_I) < 1$), Manning counterion condensation [40] around the two rods yields an ion charge per length of $\tau_I = \tau_2 - \tau_1 - 1/l_B$. When $\kappa(D-2r_I) > 1$, Manning condensation around C_2 leads to $\tau_I = \tau_2 - 1/l_B$. Since $\tau_1 \leqslant 1/l_B$, no condensation occurs around C_1. Assuming an unscreened Coulomb interaction for $\kappa(D-2r_I) < 1$ and a screened Coulomb interaction for $\kappa(D-2r_I) > 1$, one finds

$$\frac{\beta F_{\mathrm{Coul}}}{L} = \begin{cases} -\frac{2\tau_1(\tau_1 l_B+1)}{D} & \kappa(D-2r_I) < 1 \\ -\frac{2\tau_1 K_1(\kappa D)}{K_1(\kappa r_0)r_0} & \kappa(D-2r_I) > 1 \end{cases}, \qquad (3)$$

where $\beta = 1/k_BT$ and $K_1(r)$ is the modified Bessel function of the second kind, of order 1.

The rods also experience osmotic forces due to collisions with the condensed ions. We assume the ions to locate around the more highly charged C_2, with uniform contact density when rods are far apart. At close approach ($D < 2(r_0+r_I)$), a depletion zone appears where the contact density is zero in an excluded region of cross sectional area $2\delta L$, where $\delta = \sqrt{(r_0+r_I)^2 - D^2/4}$, $2r_0 < D < 2(r_0+r_I)$. The attractive depletion force associated with this excluded volume may be approximated by $\beta F_{\mathrm{dep}}/L = 2\rho_I\delta$, where the ion density is $\rho_I = \tau_I/[2\pi(r_0+r_I)l_{\mathrm{GC}}]$, and $l_{\mathrm{GC}} = (r_0+r_I)/l_B\tau_2$ denotes the Gouy-Chapman length, defined as the height above a charged surface where an ion's Coulomb energy equals its thermal energy k_BT.

In addition to depletion attraction, condensed ions around C_2 exert an unbalanced, repulsive osmotic pressure on C_1. The ion density at contact with C_1 is approximately $\rho_I e^{-\frac{z(x)}{l_{\mathrm{GC}}}}$, where $z(x)$ is the distance between the rod surfaces, at a height x above the line connecting the rod centers. Based on these considerations, the depletion and osmotic forces force per length are

$$\frac{\beta F_{\mathrm{dep}}}{L} = -\frac{2\tau_I\delta}{2\pi(r_0+r_I)l_{\mathrm{GC}}} = -\frac{\tau_2\tau_I\delta l_B}{\pi(r_0+r_i)^2}, \qquad (4)$$

$$\frac{\beta F_{\mathrm{osm}}}{L} = \frac{\tau_2\tau_I l_B}{\pi(r_0+r_I)^2}\int_{\delta}^{r_0+r_I} e^{-\frac{D-4\sqrt{(r_0+r_I)^2-x^2}}{l_{\mathrm{GC}}}}dx. \qquad (5)$$

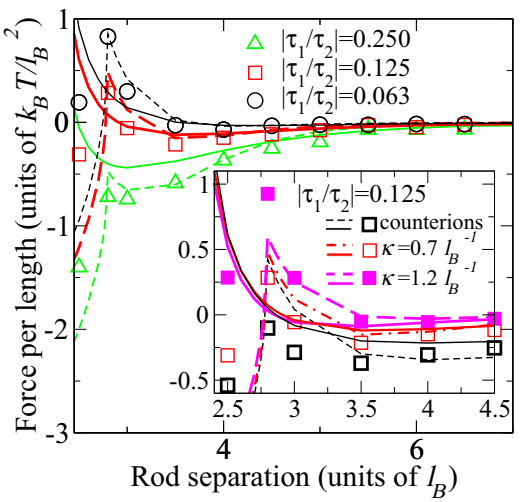

FIG. 4. The force per rod length as predicted by nonlinear Poisson-Boltzmann theory $\beta F_{\mathrm{PB}}/L$ (solid lines), condensed ion theory $\beta F_{\mathrm{IC}}/L$ (dashed lines), and simulation data (symbols), for increasing $|\tau_1/\tau_2|$ at $\kappa = 0.7l_B^{-1}$. The effect of increasing salt for $|\tau_1/\tau_2|$=0.125 is presented in the insert.

Note that the lower limit of the integration in osmotic force also takes into account the depletion zone between the macroions. The total force from the ion condensation model (IC) is then obtained by combining Eqs. (3)–(5): $F_{\mathrm{IC}} = F_{\mathrm{Coul}} + F_{\mathrm{dep}} + F_{\mathrm{osm}}$.

In Fig. 4, we compare the predictions of Poisson-Boltzmann and ion condensation models to simulation in a biologically relevant range of rod charges and ionic screening. Both theoretical models give good agreement at longer separation. However, at diminishing separation, the Poisson-Boltzmann model fails qualitatively, as it predicts a monotonic increase in force. In contrast, the IC approach accurately predicts the force peak observed via simulation, and semiquantitatively predicts the subsequent decrease in force as contact is approached. The success of the simple, IC model at close separation demonstrates the importance of properly accounting for ion depletion from the inter-rod space and the osmotic contributions to the force when the rod surface separation is on the order of one ion diameter. Indeed, depletion effects, resulting from excluded volume, are neglected in the mean-field PB theory. Weak coupling corrections to the PB theory could not yield an attraction-repulsion-attraction regime either, as they do not account for finite ion size.

Adding electrolyte enhances repulsive interactions. As observed in the Fig. 4 inset, F_{PB} is relatively unaffected by an increase of electrolyte, whereas F_{IC} follows the simulation data more accurately. In both theoretical approaches, increase of electrolyte concentration affects the force dominantly through screening (κ) and the models fail to account changes in, e.g., ion depletion due to increased ion condensation. Theoretical prediction on the critical charge asymmetry where repulsion emerges as a function of κ according to the IC model is also presented in Fig. 2.

We investigate here a coarse-grained model consisting of uniformly charged cylinders and charged spherical ions, and consider only Coulomb and hard core interactions. Effects

related to discrete solvent, chemical detail, conformational flexibility, and van der Waals interaction—all present in experimental systems—are neglected. Our work thus serves to reveal behavior whose origin is purely electrostatic and steric, and to provide a basis upon which additional effects may be included. For example, a van der Waals attraction between two cylindrical objects (see Ref. [46]) could be added to our model, and may serve to suppress the observed mid-range repulsive barriers. Solvent granularity would likely introduce a short-range depletion attraction, potentially enhancing the short-range attraction observed in our model.

IV. CONCLUSIONS

In summary, we present the first comprehensive study on the forces between oppositely and asymmetrically charged cylindrical objects in electrolyte solution. We observe conditions of pure attraction and of long-range attraction together with short-range repulsion, but our key discovery is the possibility of two free energy minima, separated by a repulsive barrier, favored at moderate charge asymmetry ($0.05 < \tau_1/\tau_2 < 0.2$) and increasing electrolyte concentration. The governing mechanism includes screened electrostatic attraction at separations exceeding the Debye length, osmotic repulsion at rod surface separations comparable to an ion diameter, and depletion attraction at separations near contact. This is in contrast to the DLVO model of charged colloids, where double minima is caused by interplay of electrostatic repulsion and van der Waals attraction. The contributions controlling the interaction are elucidated by a simple model, which proves to be superior to the nonlinear Poisson-Boltzmann equation in predicting simulated data in a biologically relevant range of parameters.

Free energy profiles within charged, macromolecular systems have important implications to many biomedical applications. We show here how a repulsive barrier may be tuned through charge asymmetry and salt concentration, how multiple attractive minima may result, and how binding strength and reversibility can be influenced. The governing physics reported here provides a valuable framework toward understanding and tuning interactions of polyelectrolytes and other rodlike objects in salt solutions, such as those involving DNA, functionalized nanotubes, membrane proteins, and viruses.

ACKNOWLEDGMENTS

We gratefully acknowledge financial support from the Academy of Finland, American Chemical Society's Petroleum Research Fund Grant No. 47776-AC5, the Aalto University School of Chemical Technology Doctoral Program, and a Marie Curie Career Integration Grant within the 7th European Community Framework Program under Grant No. 293861. Computational resources from the CSC IT Centre for Science (Finland) and the Yale University Faculty of Arts and Sciences High Performance Computing Centre (USA) are also gratefully acknowledged. Finally, we thank Dr. M. Kanduč for helpful discussion.

[1] H. Boroudjerdi, Y.-W. Kim, A. Naji, R. Netz, X. Schlagberger, and A. Serr, Phys. Rep. **416**, 129 (2005).
[2] Y. Levin, Rep. Prog. Phys. **65**, 1577 (2002).
[3] S. L. Brenner and D. A. McQuarrie, Biophys. J. **13**, 301 (1973).
[4] I. Sogami and N. Ise, J. Chem. Phys. **81**, 6320 (1984).
[5] R. Kjellander and S. Marčelja, J. Chem. Phys. **82**, 2122 (1985).
[6] Y. Jiang, Chem. Phys. Lett. **263**, 317 (1996).
[7] M. Deserno, A. Arnold, and C. Holm, Macromolecules **36**, 249 (2003).
[8] Y. Min, M. Akbulut, K. Kristiansen, Y. Golan, and J. Israelachvili, Nat. Mater. **7**, 527 (2008).
[9] N. I. Lebovka, in *Polyelectrolyte Complexes in the Dispersed and Solid State I*, Advances in Polymer Science, Vol. 255, edited by M. Müller (Springer, Berlin/Heidelberg, 2014), pp. 57–96.
[10] S. A. Palkar and A. M. Lenhoff, J. Colloid Interface Sci. **165**, 177 (1994).
[11] J. Stankovich and S. L. Carnie, Langmuir **12**, 1453 (1996).
[12] A. Lau and P. Pincus, Eur. Phys. J. B **10**, 175 (1999).
[13] J. Z. Wu, D. Bratko, H. W. Blanch, and J. M. Prausnitz, Phys. Rev. E **62**, 5273 (2000).
[14] M. Trulsson, B. Jönsson, T. Åkesson, J. Forsman, and C. Labbez, Phys. Rev. Lett. **97**, 068302 (2006).
[15] A. A. Meier-Koll, C. C. Fleck, and H. H. von Grünberg, J. Phys. Condens. Matter **16**, 6041 (2004).
[16] S. A. Safran, Europhys. Lett. **69**, 826 (2005).
[17] D. Ben-Yaakov, Y. Burak, D. Andelman, and S. A. Safran, Europhys. Lett. **79**, 48002 (2007).
[18] P. W. Debye and E. Hückel, Phys. Z. **24**, 185 (1923).
[19] B. Derjaguin and L. Landau, Acta Physicochimica USSR **14**, 633 (1941).
[20] E. J. W. Verwey, J. Phys. Colloid Chem. **51**, 631 (1947).
[21] R. R. Netz, Phys. Rev. E **60**, 3174 (1999).
[22] S. L. Brenner and V. Parsegian, Biophys. J. **14**, 327 (1974).
[23] D. Harries, Langmuir **14**, 3149 (1998).
[24] N. Kampf, D. Ben-Yaakov, D. Andelman, S. A. Safran, and J. Klein, Phys. Rev. Lett. **103**, 118304 (2009).
[25] I. Rouzina and V. A. Bloomfield, J. Phys. Chem. **100**, 9977 (1996).
[26] A. Naji, M. Kanduč, J. Forsman, and R. Podgornik, J. Chem. Phys. **139**, 150901 (2013).
[27] A. Y. Grosberg, T. T. Nguyen, and B. I. Shklovskii, Rev. Mod. Phys. **74**, 329 (2002).
[28] R. Netz, Eur. Phys. J. E **5**, 557 (2001).
[29] B. I. Shklovskii, Phys. Rev. Lett. **82**, 3268 (1999).
[30] A. Naji and R. Netz, Eur. Phys. J. E **13**, 43 (2004).
[31] M. Kanduč, J. Dobnikar, and R. Podgornik, Soft Matter **5**, 868 (2009).
[32] M. Kanduč, A. Naji, J. Forsman, and R. Podgornik, J. Chem. Phys. **132**, 124701 (2010).
[33] M. Kanduč, M. Trulsson, A. Naji, Y. Burak, J. Forsman, and R. Podgornik, Phys. Rev. E **78**, 061105 (2008).
[34] B.-Y. Ha and A. J. Liu, Phys. Rev. Lett. **79**, 1289 (1997).

[35] N. Grønbech-Jensen, R. J. Mashl, R. F. Bruinsma, and W. M. Gelbart, Phys. Rev. Lett. **78**, 2477 (1997).
[36] F. J. Solis and M. Olvera de la Cruz, Phys. Rev. E **60**, 4496 (1999).
[37] M. L. Henle and P. A. Pincus, Phys. Rev. E **71**, 060801 (2005).
[38] R. Podgornik and V. A. Parsegian, Phys. Rev. Lett. **80**, 1560 (1998).
[39] E. Allahyarov, I. D'Amico, and H. Löwen, Phys. Rev. Lett. **81**, 1334 (1998).
[40] G. S. Manning, J. Chem. Phys. **51**, 924 (1969).
[41] M. Kanduč, A. Naji, and R. Podgornik, J. Chem. Phys. **132**, 224703 (2010).
[42] V. Dahirel, M. Jardat, J. F. Dufreche, and P. Turq, Phys. Chem. Chem. Phys. **10**, 5147 (2008).
[43] E. Vuorimaa, A. Urtti, R. Seppänen, H. Lemmetyinen, and M. Yliperttula, J. Am. Chem. Soc. **130**, 11695 (2008).
[44] T.-M. Ketola, M. Hanzlíková, A. Urtti, H. Lemmetyinen, M. Yliperttula, and E. Vuorimaa, J. Phys. Chem. B **115**, 1895 (2011).
[45] D. Y. Chan and B. Halle, J. Colloid Interface Sci. **102**, 400 (1984).
[46] S. W. Montgomery, M. A. Franchek, and V. W. Goldschmidt, J. Colloid Interface Sci. **227**, 567 (2000).